Title: Liquid Metal Intrusion Testing Final Report

Author(s):   Hargather, Chelsey
              Kimberley, Jamie
              Grow, David Isaac
              Krishnamoorthy, Wish

Intended for: General distribution to academic community.

Issued: 2021-03-09

Liquid Metal Intrusion Testing
Final Report

Drs. Chelsey Hargather[*][1]**, Jamie Kimberley** [2]**, David Grow** [2]**, Wish Krishnamoorthy** [3]
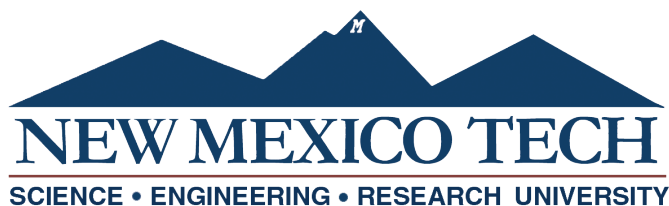[1]New Mexico Tech, Dept. of Materials Engineering
[2]New Mexico Tech, Dept. of Mechanical Engineering
[3]Qynergy, Inc., Albuquerque, NM
[*]chelsey.hargather@nmt.edu

February 8, 2018

Contents

1 Purpose

Los Alamos National Lab (LANL) is concerned about potential interactions between a tin-antimony pewter material used for localized radiation shielding and stainless-steel containers used for storage and movement of radioactive materials when containers are subjected to elevated temperatures. The specific concern is whether pewter constituents can diffuse into grain boundaries and lead to embrittlement of the stainless steel, potentially compromising the ability of stainless steel components to maintain containment. This work will provide a qualitative and quantitative understanding of the depth of penetration of the pewter coating constituents into stainless steel when the test coupons are subjected to a range of thermal environments. The results of the present work will allow LANL to determine conditions for safely using the pewter lined containers.

2 Scope

Four pewter-shielded 304 stainless steel coupons were heat treated for 30 minutes in a box furnace at the following temperatures specified by LANL: 250 °C, 475 °C, 700 °C, and 915 °C. After the heat treatment, the coupons were mounted and prepared for examination in a scanning electron microscope (SEM). SEM was used to determine:

- Existence of penetration of the pewter constituents into the grain boundaries of the stainless steel samples.

- The extent of penetration of the pewter constituents into the grain boundaries of the stainless steel samples.

- Interdiffusion between the pewter and stainless steel constituents.

3   Methodology

1. LANL provided 10 304 stainless steel test coupons and 10 lead-free pewter test coupons. Table 3.1 shows the primary constituents for the untreated 304 stainless steel and the pewter coupons.

Table 3.1: Primary constituents of the test coupons given in weight %

304 Stainless Steel	Bal: Fe	18-20% Cr	8-10% Ni	2% Mn	0.75% Mn	0.08% C	<0.02% Other
Pewter	Bal: Sn	7% Sb	1% Cu	0.006 % Pb	<1% Other		

2. The dimensions of the length, width, and height of the untreated coupons were measured. Table 3.2 displays the average dimensions and standard deviation for each of the dimensions of the stainless steel and pewter samples.

Table 3.2: Test coupon measurements

	Stainless Steel	Pewter
Length average (mm)	12.76	12.74
Length standard deviation	0.011	0.015
Width average (mm)	12.31	12.58
Width standard deviation	0.014	0.014
Thickness average (mm)	6.170	1.510
Thickness standard deviation	0.006	0.009

3. A Thermolyne Benchtop Muffle Furnace, type 47900 and an alumina capsule crucible were inspected and cleaned. The furnace is shown in Figure 3.1 below.

4. In order to baseline the furnace, a temperature profile test was performed for a target temperature of 915 °C, a ramp time of 2 hours from room temperature, and a dwell time of 1 hour at the high temperature. A NIST-traceable K-type thermocouple was inserted in the center of the furnace and a NIST-calibrated thermocouple reader was used to sample the temperature in the furnace every 5 seconds. The calibration report for the thermocouple and thermocouple reader can be found in Appendix A. The furnace used also has a built-in thermometer that was also used to record temperature data.

5. A NIST-calibrated timer was used to track the time. The calibration report for the timer can be found in Appendix B.

6. Two additional furnace baseline tests using the same temperature and furnace settings were performed to investigate the temperature profile differences between an alumina crucible and a porcelain crucible in comparison to the furnace, respectively. For each of these two tests, one thermocouple was placed in direct contact with the

Figure 3.1: A picture of the Thermolyne Benchtop Muffle Furnace, model 47900, located in 175 Jones Hall. It has a pre-drilled port for temperature monitoring and a maximum operating temperature of 1200 °C.

center of the crucible while a second was free floating in the center of the furnace and temperature readings were taken from both.

7. In order to test the metallography process and obtain an SEM baseline analysis of the pewter and stainless steel coupons, one test sample was made by sandwiching as-received stainless steel and pewter coupons that did not undergo and furnace heat treatment. The test sample was subject to the following metallographic procedure:

   (a) The sample was cold mounted using a 2:1 ratio of EpoThin 2 resin and EpoThin 2 hardener.

   (b) The sample was ground using silicon carbide grinding disks of the following grits sequentially: 80, 120, 240, 360, 600, 800, and 1200.

   (c) The sample was polished using MetaDi Supreme 0.3um diamond polish on a MicroCloth polishing cloth for twenty minutes.

   (d) The sample then went through a 20-minute ultrasonic bath with isopropyl alcohol using a Branson 1800 machine.

8. Scanning electron microscope (SEM) and energy-dispersive X-ray spectroscopy (EDS) analyses were performed on the sample using a Hitachi S-4100 SEM.

9. For preparation of the coupons being subject to heat treatment, the following cuts were made using a Buehler Isomet diamond saw and cutting fluid:

4

(a) 2 pewter coupons were cut into quarters for placement on top of the stainless steel coupons.

(b) 4 stainless steel coupons were cut in half lengthwise.

10. Coupon testing process for all four target temperatures were performed according to the following procedure:

(a) An alumina crucible was placed in the furnace at ambient temperature.

(b) A thermocouple was assigned to the alumina or porcelain crucible while a second was placed at the center of the furnace.

(c) Furnace was ramped up to the desired temperature. Table 2 shows the furnace settings for the target temperatures and the location of the corresponding datasheets in the appendices.

Table 3.3: Thermolyne Benchtop Muffle Furnace settings

Sample #	Temperature	Ramp Time (hr)	Heat treatment time (hr)
1A	250 °C	0.5	0.5
1B	250 °C	0.5	1
2	475 °C	1	0.5
3	700 °C	1.5	0.5
4	915 °C	2	0.5

(d) Once the target temperature on the furnace was reached, the crucible was subjected to 10 minutes of dwell time at the target temperature.

(e) The furnace was then opened swiftly and a quarter of a pewter coupon was placed on top of an entire SS coupon and together they were placed in the center of the alumina or porcelain crucible.

(f) Once the furnace reached the target temperature after coupon insertion, the heat treatment time period began and time was recorded with a NIST-traceable stopwatch.

(g) After the necessary time at the target temperature, the test coupons were removed from the furnace and the samples were allowed to cool to ambient temperature.

11. A Buehler Isomet diamond saw cutter and Buehler cutting fluid were used to cut each test coupon after it cooled to ambient temperature. Figure 3.2 is a diagram showing the direction that the four coupons tests were cut. The gray circular outline represents the pewter and the dashed line represents the pathway of the diamond saw. The solid box represents the treated stainless steel.

12. One half of the cross-sectioned sample was sandwiched with an untreated stainless steel coupon and treated with the same metallography procedure as in step 7.

13. After sample preparation was complete, SEM and EDS analysis was completed with the Hitachi S-4100.
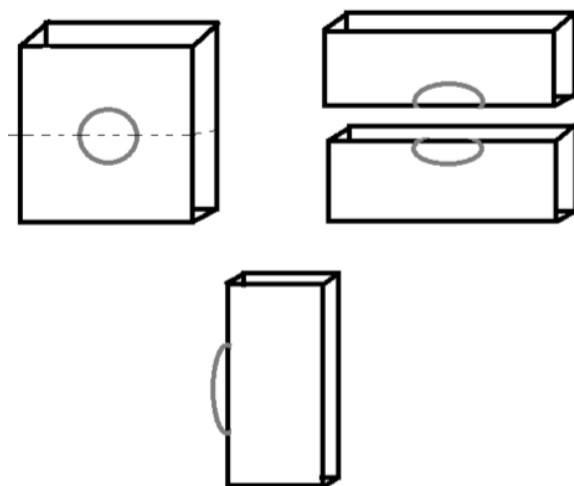
Figure 3.2: Cutting orientation of treated stainless steel and pewter coupons sandwiched together. The dashed line signifies the pathway of the diamond blade.

4 Results and Discussion

4.1 Furnace baseline test results

The first baseline temperature test performed in the furnace was a 2 hour temperature ramp-up time to compare the reading from the NIST-traceable thermocouple to the temperature provided by the furnace. The furnace door being opened for sample insertion was simulated. The temperature history data from the first baseline temperature test are shown in Appendix C, Figure C1. The data show consistent readings between the furnace temperature and the thermocouple after the first 20 minutes of ramp up.

The graphs in Appendix C, Figures C2-C3 show the baseline temperature histories for the alumina and porcelain crucible tests compared to the relative furnace temperature, respectively. For each of these tests, two thermocouples were inserted into the furnace, one touching the crucible and one floating in the central furnace chamber. Figure C2 shows that alumina crucible and the furnace ramped up to the target temperature at a nearly equal rate. After the furnace was opened and closed to simulate the sample insertion (time ~130 min), the furnace recovered the target temperature more quickly than the crucible. Air cooling of the furnace was completed by opening the furnace door and allowing the furnace to cool. The thermocouples were left in their original positions. Figure C2 shows that the alumina crucible cooled more quickly than the internal temperature of the furnace.

Figure C3 shows the baseline temperature history for the porcelain crucible. The data show that unlike the alumina crucible, the porcelain crucible heated at a slower rate than the furnace, and did not cool to the same temperature as the furnace during the simulation of the sample insertion. During cooling, the porcelain crucible cooled at a much slower rate than the internal temperature of the furnace.

It should be noted that there was up to a ± 10 °C difference between the crucibles and furnace readings, as the variation in the temperature readings was about ± 5 °C.

4.2 Coupon Treatment Results

4.2.1 250 °C test

The temperature profile graph for the heat treatment of Sample 1A is shown in Appendix D Figure D1. Figure D1 shows Sample 1A during its furnace heat treatment at 250 °C for 30 minutes, where the red squares indicate the temperature of the crucible and the blue circles indicate the temperature of the furnace. The crucible for Sample 1A did not reach the set furnace temperature before sample insertion, and peaked around 230 °C towards the end of the test. Sample 1A showed no metallurgical interaction after being subject to the target temperature for the required 30 minutes. This is likely due to the melting temperature of the pewter being at or around 240 °C.

The dwell time in the furnace time was increased from 30 minutes to 1 hour for Sample 1B to see if a longer time period would initiate a metallurgical interaction. The temperature profile graph for the heat treatment of Sample 1B is shown in Appendix D Figure D2. It is to be noted that sample 1B's crucible never reached the set furnace temperature, and reached a peak temperature of about 230 °C towards completion of the test. After 1 hour of heat treatment at 250 °C, the pewter had not melted and no metallurgical interaction took place. The only observable change in either sample was in the pewter. After being in the furnace at 250 °C it turned from a gray color to a bronze color, also demonstrated in Figure 4.1.
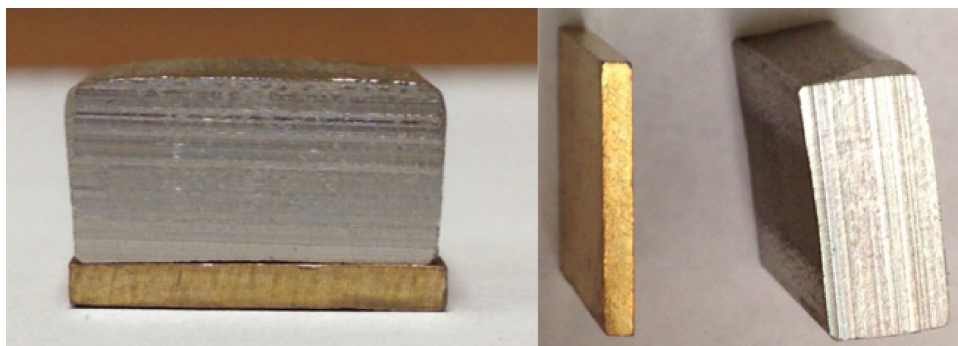

Figure 4.1: Photographic images of Sample 1B after undergoing furnace heat treatment for 60 minutes at 250 °C.

The metallography procedure, SEM analysis, and EDS analysis were not performed on either 250 °C sample due to the observed lack of large-scale interaction between the stainless steel and pewter.

4.2.2 475 °C test

The following results are for Sample 2, which was heat treated in the furnace at 475 °C for 30 minutes. The temperature history profile is shown in Appendix D Figure D3. Figure D3 indicates that Sample 2's crucible reached the target temperature during heat treatment about 8 minutes after sample insertion, but the jump in temperature around 3000 seconds indicates that the thermocouple may have lost contact with the crucible. Upon removal from the furnace, it was observed that a weak metallurgical bond had formed between the treated pewter and stainless steel coupons. During the sectioning of Sample 2, the pewter coupon detached from the stainless steel coupon. To investigate the extent, if any, of the metallurgical interaction between the pewter constituents and the stainless steel, the stainless steel half of Sample 2 was mounted against an untreated stainless steel coupon and grinded, polished, and ultrasonically cleaned. SEM and EDS was performed to investigate any signs of diffusion between of pewter constituents into the stainless steel. In this section and in the remainder of the document, the EDS line scans shown start from the tail end of the red arrow in the SEM image and end at the tip of the arrowhead.
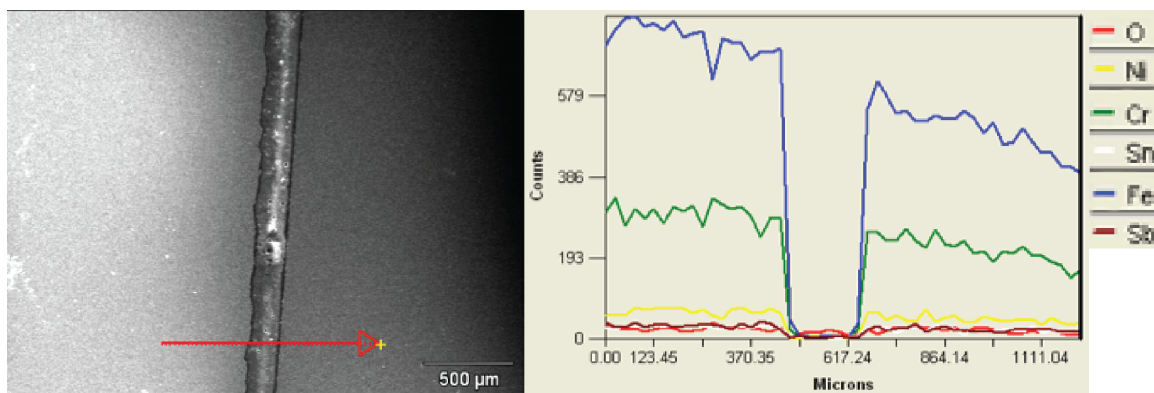

Figure 4.2: SEM image and EDS line scan of Sample 2, after undergoing furnace heat treatment at 475 °C for 30 minutes.

Figure 4.2 shows the interface between the untreated stainless steel (left) and heat-treated stainless steel (right). The gap between the untreated and treated samples filled with epoxy during the mounting procedure. The EDS line scan shows that there is little to no trace of the pewter constituents, tin and antimony, and a high presence of iron and chromium in both the treated and untreated stainless steel. The non-constant counts of iron and chromium leading into and out of the epoxy interface are likely due to a large beam spot size on the SEM. The variation in absolute value of the elemental counts is not due the amount of iron and chromium is increasing or decreasing as the interface is approached. In conclusion, there are no signs of a metallurgical interaction having taken place between the pewter and 304 stainless steel in Sample 2 after 30 minutes of heat treatment.

4.2.3 700 °C test

The temperature history profile for Sample 3, heat treated for 30 minutes at 700 °C, is shown in Appendix D Figure D4. Figure D4 indicates that Sample 3's crucible reached the target temperature about 15 minutes after sample insertion. When Sample 3 was removed from the furnace, there was evidence of adhesion between the pewter and the stainless steel. The treated coupon of bonded pewter and stainless steel was mounted (for SEM analysis) with an untreated sample of stainless steel, such that the pewter was sandwiched between the untreated stainless steel and the treated stainless steel that it was bonded to.
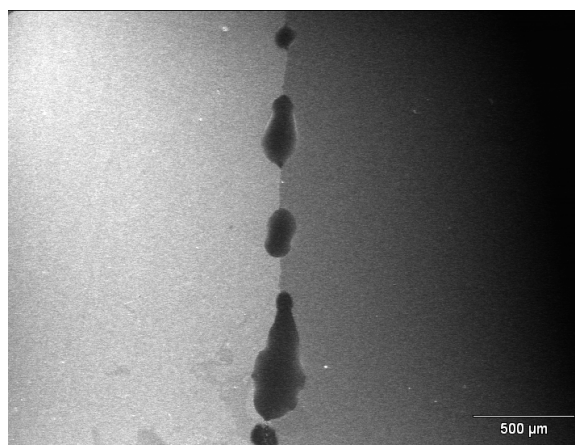
Figure 4.3: SEM image of Sample 3, after undergoing furnace heat treatment at 700 °C for 30 minutes, with the light-gray pewter on the left, and the dark-gray stainless steel on the right.

Figure 4.3 shows the interface of the treated pewter and treated stainless steel, where the lighter area to the left is the pewter and the darker area on the right is the stainless steel. The beginnings of the formation of a metallurgical bond between the treated pewter and stainless steel coupons are evident. The interface consists of fused areas wherein the pewter and stainless steel are in intimate contact and areas where the pewter and stainless steel are separated by voids/bubbles.

Figure 4.4 shows the interface of Sample 3 at a higher magnification. While Figure 4.3 showed indications of regions with the beginnings of a metallurgical bond, The EDS line scans in Figure 4.4 indicate no clear exchange of constituents across the interface. The sloped region in the plot corresponding to the boundary between the pewter and stainless steel is likely an artifact of averaging occurring due to the SEMs beam size. Thus, we cannot definitively say that a metallurgical bond has formed. The only conclusion that can be drawn is that there is intermittent adhesion in Sample 3 between the 304 stainless steel and the pewter that forms as a result of 30 minutes of heat treatment at 700 °C.
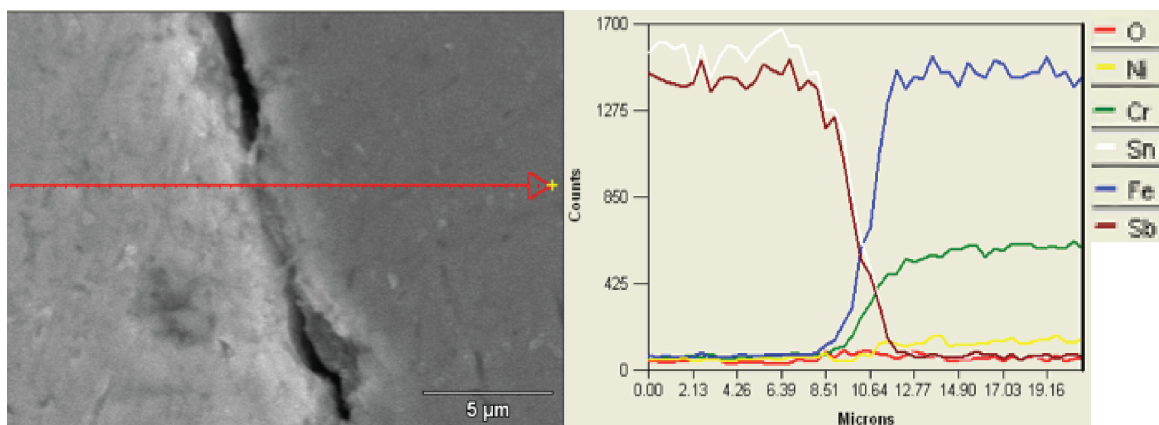
Figure 4.4: SEM image and EDS line scan of Sample 3, across an area showing adhesion between the pewter and stainless steel.

4.2.4 915 °C test

The following results are for Sample 4, which was treated at 915 °C for 30 minutes. The temperature history profile for Sample 4 is given in Appendix D Figure D4. The temperature history profile indicates that the crucible containing Sample 4 did reach the target temperature just before sample insertion, and regained the target temperature immediately after sample insertion.

Figure 4.5 (a) depicts the 915 °C sample after undergoing a furnace heat treatment for 30 minutes. The treated stainless steel is on the left and the lighter gray pewter that formed a droplet shape is centered in the image. A large crack runs between the original interface of the stainless steel and the pewter that might have occurred during cooling. The untreated stainless steel is visible at the very right hand side of the image. An important observation that can be made from Figure 4.5 (a) is that during the heat treatment, the pewter constituents diffused into the stainless steel. This conclusion is drawn because there is a region of about 250-350 μm, of lighter gray pewter constituents that are to the left of the crack showing the original interface between the pewter and the stainless steel. This region will be referred to as the melt affected zone (MAZ).

A higher contrast image of Sample 4, focusing on the various layers of the pewter droplet after re-solidification, is shown in Figure 4.5 (b). The increased contrast of Figure 4.5 (b) shows that several distinct layers have evolved within the microstructure during the heat-treating and subsequent cooling processes. The layers are numbered, ranging from the MAZ (Layer 5) to a surface oxide (Layer 1). The next section will discuss the elements and phases present in each of the layers based on EDS line scans.

Figure 4.6 shows SEM images and the corresponding EDS line scans across the five different layers labeled in Figure 4.5 (b) above. Figure 4.6 (a) scans the edge of pewter closest to the furnace environment through Layer 1 and Layer 2, Figure 4.6 (b) scans through the inner layers, Layer 2 and Layer 3 of pewter, and Figure 4.6 (c) scans through additional

10
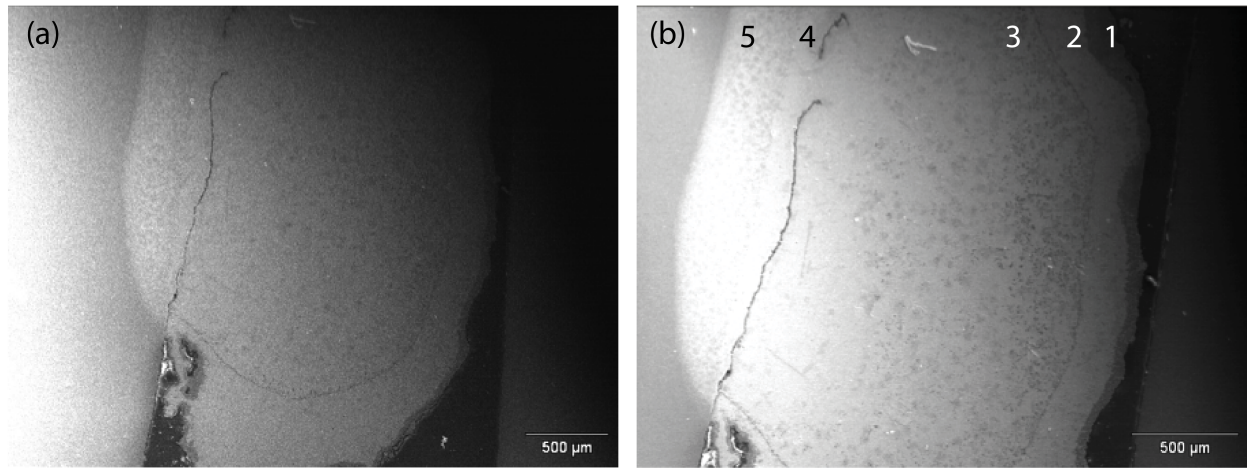
Figure 4.5: SEM image of Sample 4 after undergoing furnace heat treatment at 915 °C for 30 minutes, showing the re-solidified pewter.

inner layers of the pewter, Layer 3 and Layer 4, followed by scanning the MAZ, and the scan ends within the treated stainless steel. Additional line scans performed at higher resolutions can be found in Appendix E. It should be noted that the line scans begin at the tail of the arrow and end at the point of the arrow, while the line scans are shown in reverse; they begin at the 0 micron point on the x-axis and move right. The relative ratios between the various constituents should be examined, rather than quantitative counts of the constituents present.

Figure 4.6 (a) begins in Layer 1 and ends in Layer 2. The associated line scan shows that Layer 1 is primarily iron (red line). Oxygen (red line), tin (white line), and antimony (brown) are also present in Layer 1. It should be noted that this surface layer, Layer 1, is the only region where there is a noticeable oxygen presence in the treated sample. As the interface in the line scan between Layer 1 and Layer 2 is passed, Layer 2 emerges as a tin and antimony rich region. It is likely that upon heating and subsequent cooling, Layer 2 becomes depleted in iron as the iron oxide layer is formed across the surface of the melted pewter. In conclusion, Figure 4.6 (a) demonstrates that Layer 1 is an iron oxide layer, and Layer 2 is an antimony- and tin-rich layer.

Furthermore, EDS point scans were performed in Layer 1 and Layer 2 to confirm the predicted constituents present in each layer and are shown in Figure 4.7. Since the layers appear to consist of multiple phases, a point scan would be more accurate in determining the constituents in each phase. The line scan within a layer only provides an overview of the elements present in it and does not give an indication of their distribution within the layer.

Figure 4.7 (a) shows an SEM image detailing the locations of point scans that were performed in this region. Figure 4.7 (b) shows the results from the point scan at Point 1 (dark area), which is located in Layer 1, the iron oxide region. The point scan shows that the pri-
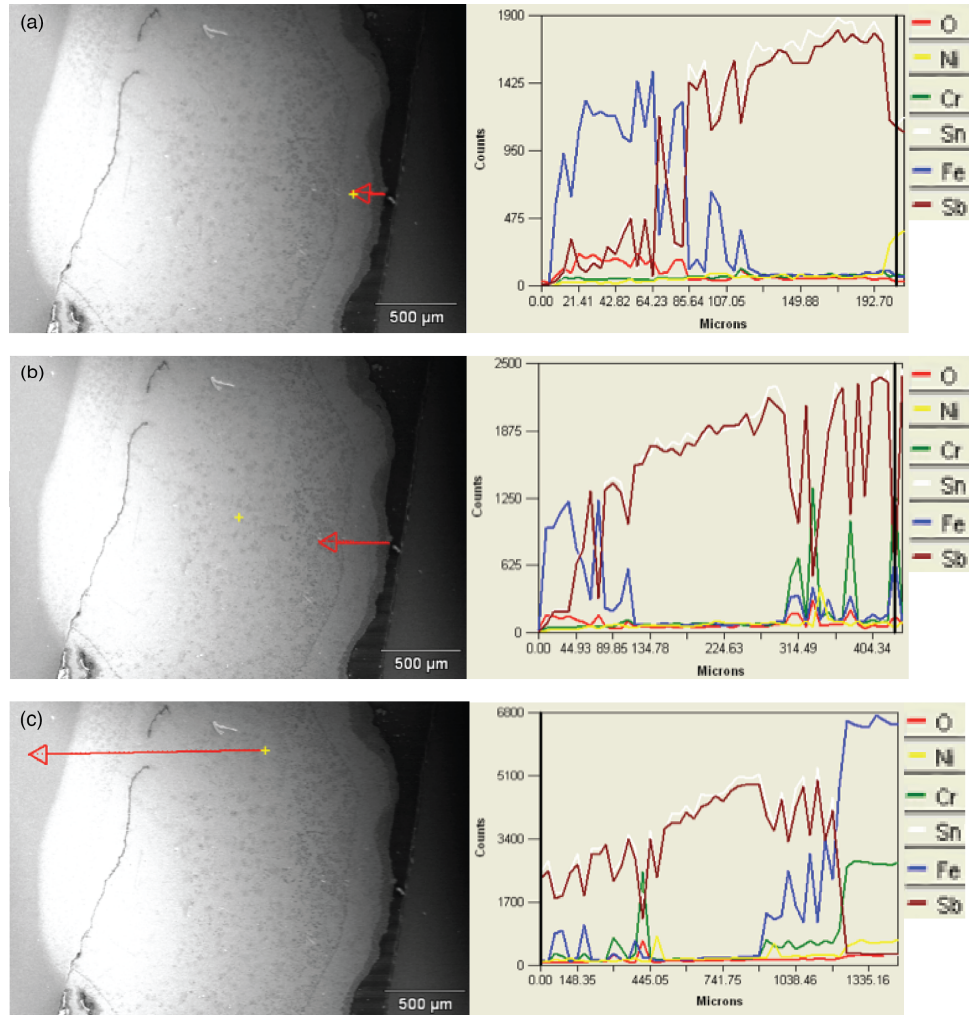
Figure 4.6: SEM image and corresponding EDS line scan Sample 4 showing: (a) edge of pewter closest to the furnace environment, (b) inner layers of pewter, and (c) inner layers of the pewter, the MAZ, and ending within the treated stainless steel.

mary element identified in this region is iron. Oxygen, tin, and antimony are also present. The presence of tin and antimony makes sense, as this region was originally 100% pewter as evidenced by the point scan in the light area (Point 3) which contains only tin and antimony. Also, some residual tin and antimony could have been picked up from the surrounding area and the dark region could very well be iron oxide. During heat treatment, iron diffused through the entire pewter melt and eventually formed an oxide layer at the surface while exposed to air. The formula for the iron oxide could not be determined since calibrated elemental standards were not available for quantitative estimation of the composition.
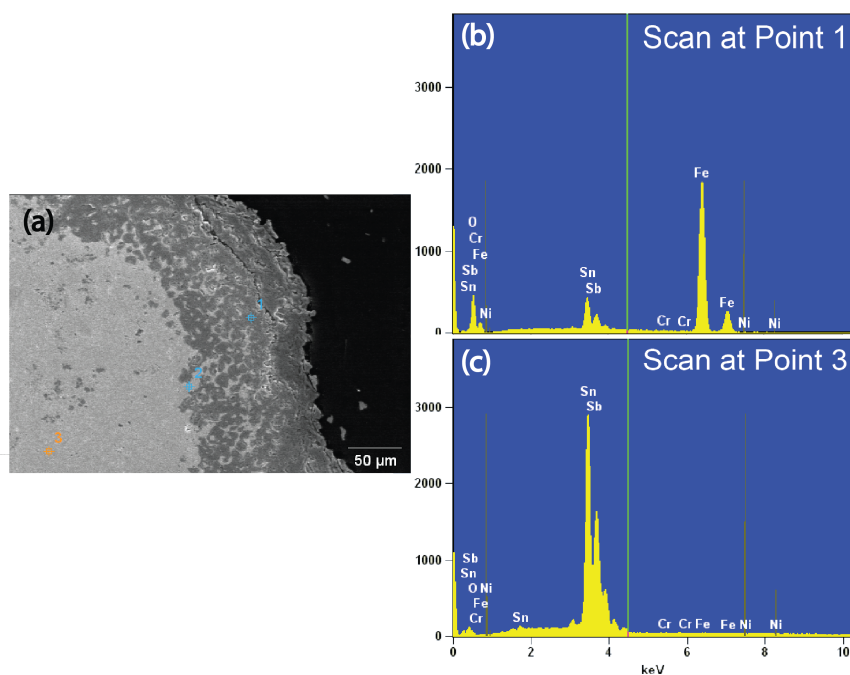

Figure 4.7: (a) EDS point scan of Sample 4, with reference from the layers identified in the line scan from Figure 4.6 (a). (b) shows a point scan from Point 1 in the iron oxide region and (c) shows a point scan from Point 3 above in the tin and antimony rich region.

The SEM image in Figure 4.6 (b) shows a line scan that begins on Layer 1, passes through Layer 2, and ends in Layer 3. The EDS line scan results from Figure 4.6 (b) show 3 distinct regions: Layer 1, the iron oxide region with some tin and antimony present, Layer 2, a tin and antimony rich region, and layer 3. From this first line scan, Layer 3 appears to be a two- or three- phase region, where one region is rich in tin and antimony and one is rich in chromium. Figure 4.8 shows an enlarged region of Layer 3, and shows more clearly that Layer 3 is actually a three-phase region. Region 1 appears as light gray and is likely a solution phase, Region 2 appears as medium gray and is likely a solution phase, and Region 3 are precipitates that appear as dark gray.
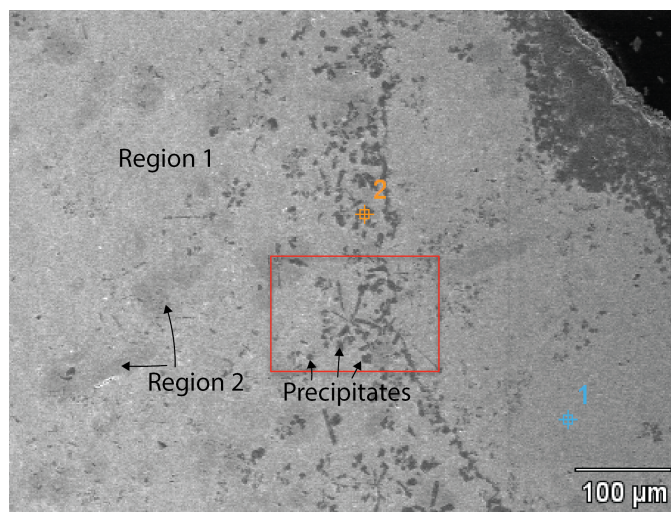
Figure 4.8: SEM image Sample 4, showing Layer 1, Layer 2, and Layer 3, which was treated at 950 °C. This image shows that Layer 3 consists of 3 phases: 2 separate solution phases (light and medium gray) and a precipitate phase (dark gray).

If the area inside the red box in Figure 4.8 is imaged at higher resolution, the three regions present in Layer 3 become more evident. Figure 4.9 shows (a) an SEM image of that region of Layer 3 with point scans that are performed at points labeled 1, 2, and 3. Figure 4.9 (b) shows the point scan at Point 1, which is in the precipitate region. The point scan data shows that the precipitate region, Region 3, in Layer 3 is primarily chromium and oxygen, with a lesser amount of iron appearing. This precipitate can be designated as chromium/iron oxide. Figure 4.9 (c) shows the medium gray region from Point 2, identified as Region 2 in Figure 4.8. This region shows constituents from both the pewter and the stainless steel phases; with appreciable amounts of iron, chromium, tin, and antimony being identified in the line scan. Figure 4.9 (d) represents the point scan data from Point 3, the light gray region Layer 3 identified as Region 1 in Figure 4.8 . Region 1 is a tin and antimony rich region, with negligible amounts if any stainless steel constituents identified in this point scan. In summary, Layer 3 consists of a three-phase region, a pure tin and antimony phase (that could be pewter), a phase containing tin, antimony, iron and chromium, and a precipitate phase of iron and chromium oxide. The precipitates were likely formed during cooling.
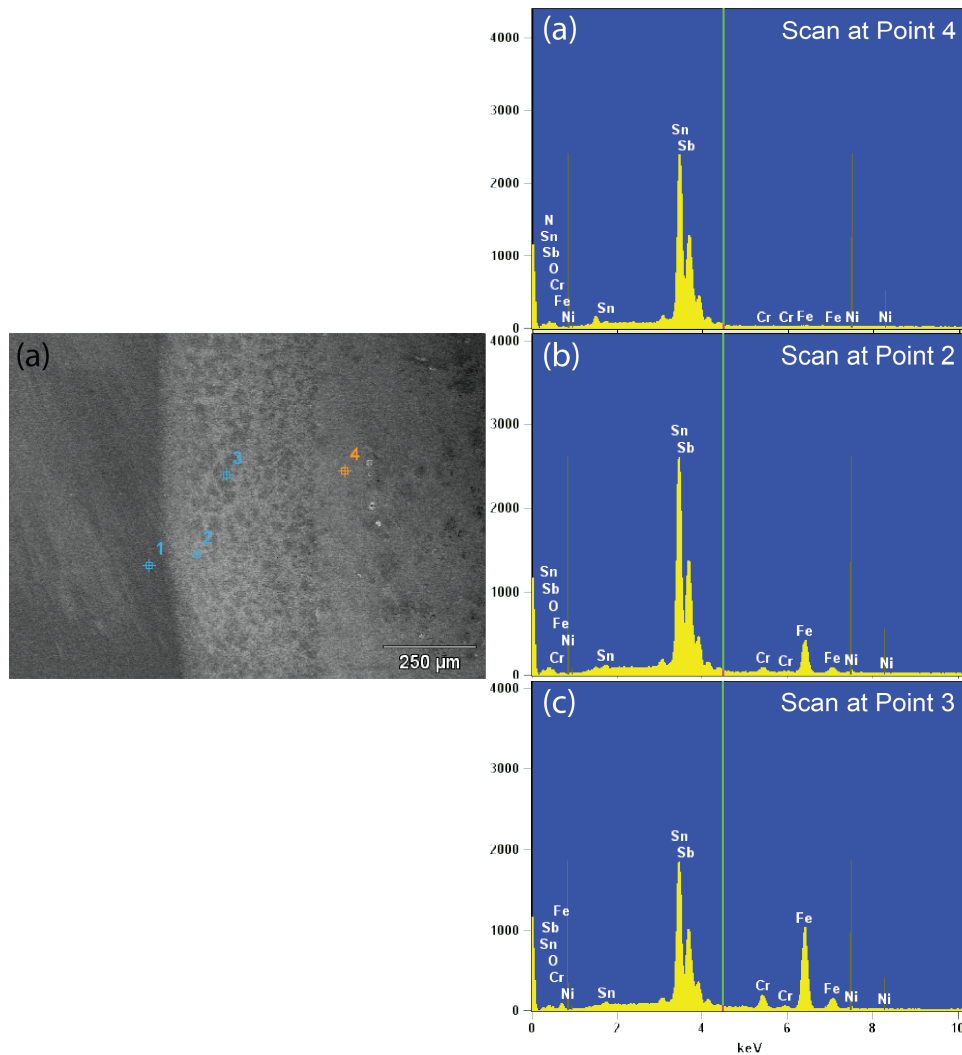
14
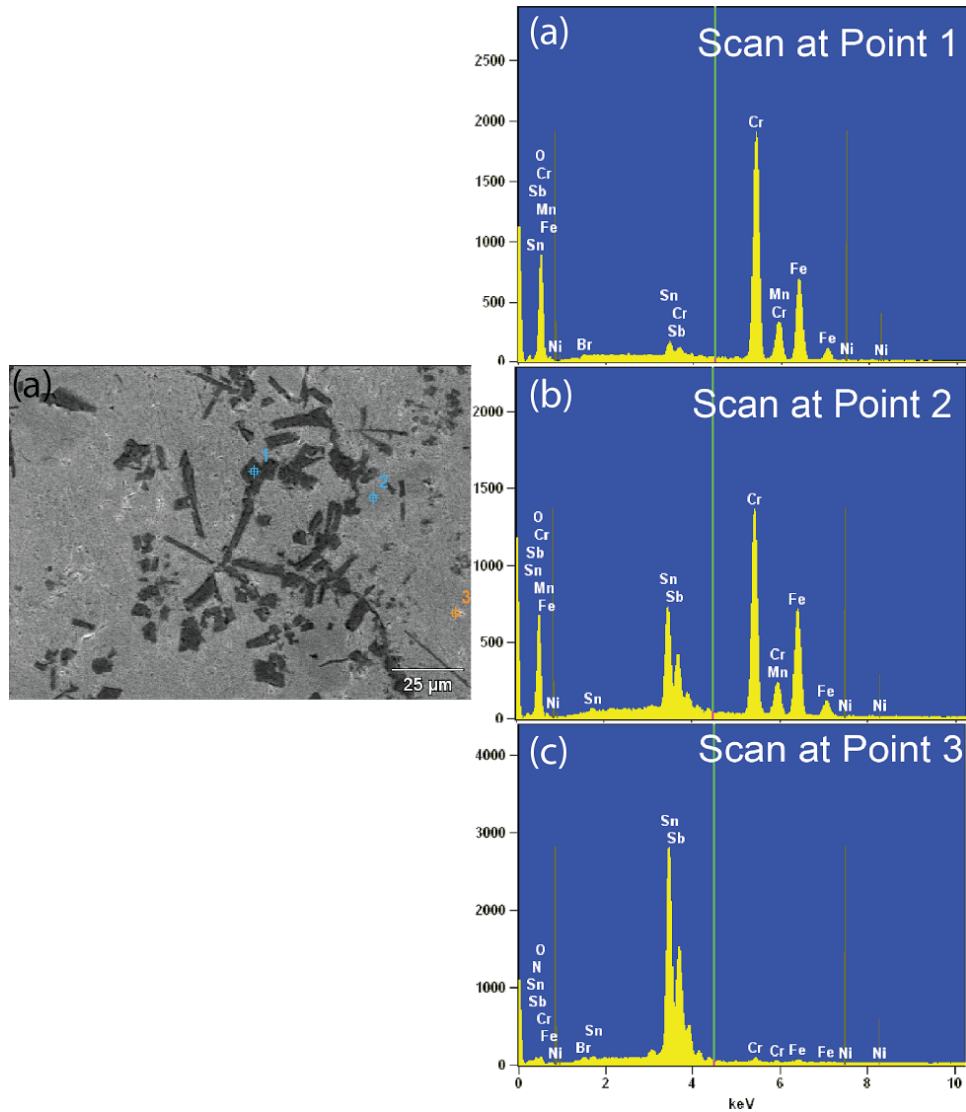
Figure 4.9: (a) Higher resolution SEM image of Sample 4, showing Layer 3 with point scans performed at labels 1, 2 and 3. (b) EDS point scan at Point 1, (c) EDS point scan at Point 2, (d) EDS point scan at Point 3.

Finally, the SEM image from Figure 4.6 (c) begins in Layer 3, the 3-phase region, passes through Layer 4, then through Layer 5, the melt affected zone (MAZ), and ends in the treated stainless steel. After passing through Layer 3, the 2-phase region with chromium precipitates, Layer 4 is analyzed. Layer 4 is clearly a region rich in antimony and tin, and no stainless steel constituents are present in the line scan data. As Layer 5, the MAZ is entered, it is clearly another two-phase region, one rich in the pewter constituents, tin and antimony, and the other rich in stainless steel constituents, iron and chromium. As the line scan leaves Layer 5, we see only iron, chromium, and nickel identified, indicating that the line scan completed in pure stainless steel. In conclusion, Figure 4.6 (c) identifies Layer 4 as a tin and antimony rich region depleted of stainless steel constituents, and

Layer 5, the MAZ, is a two-phase region, where one phase is rich in tin and antimony, and one phase is rich in iron and chromium.

To confirm the conclusions made about the constituents present in Layer 4 and Layer 5, additional point scans were performed within each region present in Layer 4 and Layer 5, and the results are presented in Figure 4.10. Figure 4.10 (a) shows the SEM image with the light gray Layer 4, labeled as Point 4; Layer 5, which is a two-phase region shows points labeled 2 and 3, and finally the dark gray region labeled Point 1, which is stainless steel. The point scan in Figure 4.10 (b) represents the light gray region of Layer 4, which the line scans showed to be a region rich in tin and antimony. The point scan confirms this assessment, showing that Layer 4 has no measurable stainless steel constituents such as iron or chromium.

Figure 4.10: (a) Higher resolution SEM image Sample 4, showing Layer 4 and Layer 5 with point scans performed at Points 1, 2, 3, and 4. (b) EDS point scan at Point 4, (c) EDS point scan at Point 2, (d) EDS point scan at Point 3.

The point scans shown in Figure 4.10 (c) and Figure 4.10 (d) are both in Layer 5, the MAZ. As mentioned in Figure 4.5, the MAZ is of interest because it shows that upon melting of the pewter, pewter constituents entered into the stainless steel matrix. It is also worth mentioning that as the sample air cooled from the outside surface inward, the MAZ would be the last region of the treated sample to solidify and cool. Since the penetration and distribution of the pewter constituents had progressed substantially by the end of the 30-minute experiment, the transport mechanism (i.e. did the pewter enter the stainless steel along the grain boundaries and then disperse, or some other method) of the pewter constituents through the stainless steel cannot be determined. In can be concluded that after 30 mins the diffusion into the SS is limited to a few hundred microns.

Figure 4.10 (c) and Figure 4.10 (d) show that the MAZ is clearly a 2-phase region. The point scan in Figure 4.10 (c) is in the lighter phase of the MAZ that appears to be the matrix phase, and the results indicate that it is primarily pewter constituents of antimony and tin. A point scan of the darker, second phase is scanned in Figure 4.10 (d) at Point 3, and shows constituents from both the pewter and the stainless steel, mainly antimony, tin, and iron. An additional scan that is more clearly located on the darker second phase region may be necessary to conclude that this is a two-phase region.

In conclusion, we have identified 5 layers with varying phases present as a results of Sample 4 undergoing a furnace heat treatment at 915 °C. Table 4.1 summarizes the layers and their constituents.

Table 4.1: Summary of the constituents present in each layer of Sample 4 after undergoing a furnace heat treatment at 915 °C.

Layer	Phase	Constituents	Description
Layer 1	1 (dark)	Fe & O, some Sn & Sb	Iron oxide
Layer 2	1 (light)	Sn & Sb	
Layer 3	1 (light)	Sn & Sb	
	2 (med)	Fe, Cr, Sn, Sb	
	3 (dark)	Cr, O, some Fe	Cr or Fe oxide precipitate
Layer 4	1 (light)	Sn & Sb	
Layer 5	1 (light)	Sn & Sb	Melt Affected Zone (MAZ)
	2 (dark)	Fe, Sn, & Sb	

From the analysis done in the present work, a model of how each of the Layers identified in Table 4.1 can be developed. As Sample 4 is heated, the pewter starts to melt. The tin and antimony constituents from the lead-free pewter penetrated the stainless steel across the original stainless steel-pewter interface, creating the MAZ. Iron and chromium constituents then leave the MAZ and become distributed throughout the pewter melt. As the iron from the pewter melt reaches the surface of the pewter sample, an oxide layer (Layer 1) is formed. Upon cooling, additional layers form. Layer 2 forms below Layer 1 and is rich in tin and antimony, as the iron present has segregated to the surface to

form the oxide. Layer 3 forms next and consists of 3 phases: a tin and antimony solution phase, an iron, chromium, tin, and antimony solution phase, and a precipitate phase consistent of chromium and oxygen with some iron. Under Layer 3 forms Layer 4, a layer rich in tin and antimony with almost no trace of stainless steel constituents present. This is likely a depleted region that was the result of iron and chromium constituents dispersing throughout the pewter melt. Finally, Layer 5, the MAZ, is a two-phase region, one rich in pewter constituents and one rich in stainless steel constituents. This process is represented schematically in Figure 4.11 below.
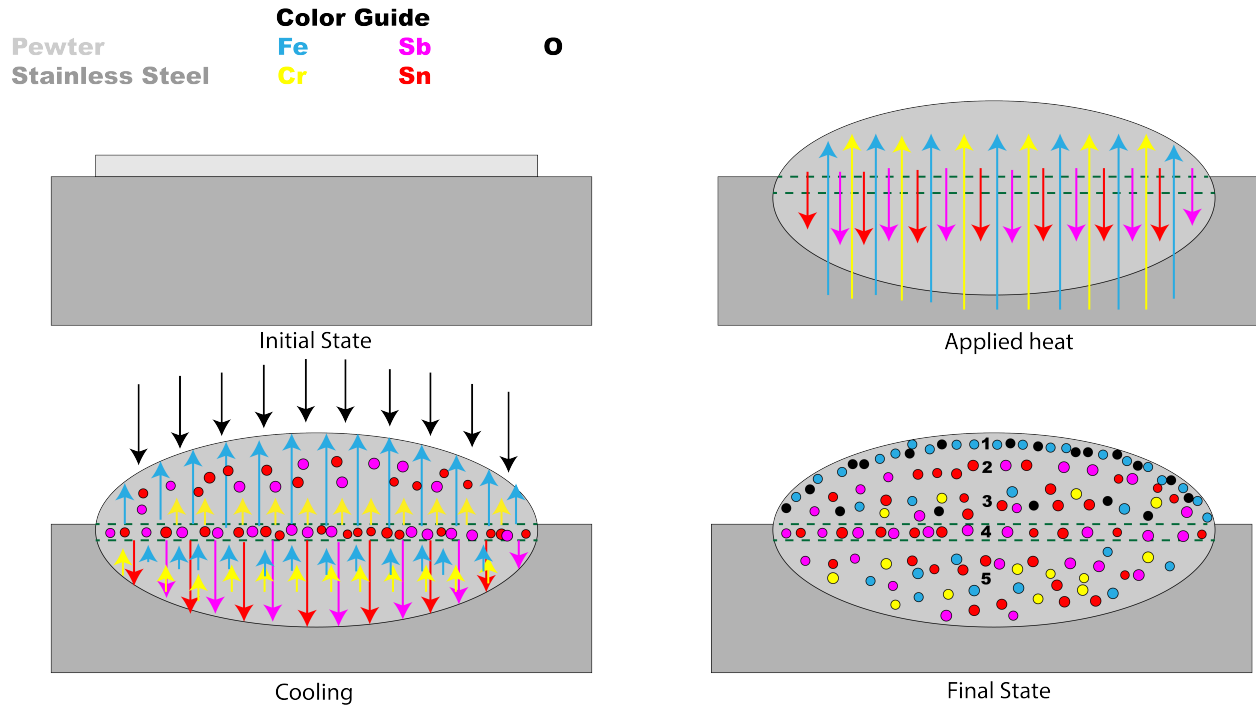
Figure 4.11: Schematic diagram of the evolution of the microstructure of Sample 4 after it was subject to a 30 minute heat treatment at 915 °C for 30 minutes, and then air cooled. The Layers 1-5 that were identified in Table 4.1 are labeled numerically in the Final State.

5 Conclusions

Key findings from this project include:

1. For 30 minutes of exposure time, no metallurgical interaction took place between stainless steel and the lead-free pewter at 250 °C or 475 °C.

2. For 30 minutes of exposure time at 700 °C, intermittent adhesion appeared between the 304 stainless steel and the lead-free pewter. Based on the experiments performed, the formation of a metallurgical bond or exchange of pewter and 304 stainless steel constituents cannot be confirmed.

3. For 30 minutes of exposure time, the critical temperature for interaction to occur between 304 stainless steel and the lead-free pewter (comprised primarily of tin and antimony) is greater than 700 °C.

4. At 915 °C, stainless steel constituents were transported into the pewter and *vice versa*, resulting in a metallurgical bond. The penetration depth of the pewter constituents into the 304 stainless steel is between 300 - 400 μm.

   - The mechanism of penetration of the pewter constituents into the 304 stainless steel (*e.g.* via grain boundaries) cannot be determined from the experiments performed.
   - No obvious intergranular penetration is occurring in the MAZ.

5. A preliminary model for the microstructural evolution between pewter and 304 stainless steel at 915 °C is developed and summarized in the following stages:

   (a) As the pewter melts, the tin and antimony constituents from the lead-free pewter penetrated the stainless steel creating the MAZ

   (b) Iron and chromium left the MAZ and distributed throughout the pewter melt

   (c) As the iron reached the surface of the pewter exposed to air, an iron oxide layer formed

   (d) Upon cooling, 5 distinct layers evolved within the pewter melt and the MAZ. From the surface down they were as follows:

       i. A surface iron oxide layer
       ii. An underlying layer consisting of only tin and antimony. This layer may have formed upon cooling when iron segregated to the surface to form the oxide
       iii. A third layer beneath consisting of 2 phases, a pure tin and antimony phase and a tin, antimony, iron and chromium phase, along with chromium and iron oxide precipitates
       iv. A fourth layer underneath that appeared to be zone depleted of iron and chromium, consisting of only tin and antimony

     v. A fifth layer in the original stainless steel, the melt affected zone, consisting of a fine grained microstructure with 2 phases one richer in iron and chromium than the other.

6. There is no evidence of intergranular penetration of pewter constituents into the stainless steel grain boundaries after 30 minutes of exposure time at temperatures up to 915 °C, meaning the 304 stainless steel is not facing embrittlement due to the melting of the pewter constituents

6 Recommendations

Based on the conclusions from the experiments performed, the following recommendations can be made:

- Further investigation of the microstructural evolution of the 304 stainless steel and pewter interaction will allow for a quantitative estimate of the MAZ formation and evolution. A time-temperature study needs to be completed at intermediate temperatures between 700 °C and 915 °C and in time increments as short as 5 minutes.

  - Information on the mechanism of penetration of the pewter constituents into the stainless steel would be obtained from this future work

- Charpy or izod test coupons can be machined out of 304 stainless steel and heat treated with pewter (as in this study) at different temperatures and times and tested to evaluate quantitatively estimate any change in mechanical properties of the stainless steel

- Other materials in the glove box other than stainless steel should be investigated for the penetration of pewter constituents in a fire scenario.

7 Acknowledgements

Appendix A   Thermocouple and thermocouple reader documentation

INNOCAL®
INNOVATIVE CALIBRATION SOLUTIONS

625 East Bunker Court
Vernon Hills, Illinois 60061
PH: 866-466-6225
Fax: 847-327-2993
www.innocalsolutions.com

NIST Traceable
Calibration Report

Cole-Parmer
625 E Bunker Court
Vernon Hills, IL 60061 United States

Manufacturer:	Digi-Sense	**Calibration Date:**	06/07/2017
Model Number:	20250-02	**Calibration Due Date:**	
Description:	Thermometer, Digital Dual	**Condition As Found:**	Initial Calibration
Asset Number:	CP254768	**Condition As Left:**	In Tolerance, No adjustment
Serial Number:	161213784		
Procedure:	DS Digi-Sense 20250-02		

Remarks:
NIST-traceable calibration performed on the unit referenced above in accordance with customer requirements, published specifications and the lab's standard operating procedures. No adjustments were made to the unit.
Recommended calibration due date is 12 months from date of purchase.

Standards Utilized

Asset No.	Manufacturer	Model No.	Description	Cal. Date	Due Date
CP50148	Fluke Corporation	5522A	Calibrator, Multifunction	10/06/2016	10/31/2017

Calibration Data

FUNCTION TESTED	Nominal Value	As Found	Out of Tol	As Left	Out of Tol	CALIBRATION TOLERANCE
Input 1 Temperature Simulation Type K	-190.0 °C Type K	-188.2		Same		-192.9 to -187.1 °C Type K [EMU 0.34 °C[TUR 8.8:1]
I	0.0 °C Type K	0.7		Same		-1.0 to 1.0 °C Type K [EMU 0.17 °C[TUR 5.9:1]
I	500.0 °C Type K	500.6		Same		496.5 to 503.5 °C Type K [EMU 0.27 °C[TUR 13:1]
I	990.0 °C Type K	990.8		Same		984.1 to 995.9 °C Type K [EMU 0.27 °C[TUR 22:1]
I	1350.0 °C Type K	1351		Same		1342.3 to 1357.7 °C Type K [EMU 0.4 °C[TUR 19:1]
Input 2 Temperature Simulation Type K	-190.0 °C Type K	-188.5		Same		-192.9 to -187.1 °C Type K [EMU 0.34 °C[TUR 8.8:1]
I	0.0 °C Type K	0.6		Same		-1.0 to 1.0 °C Type K [EMU 0.17 °C[TUR 5.9:1]
I	500.0 °C Type K	500.7		Same		496.5 to 503.5 °C Type K [EMU 0.27 °C[TUR 13:1]
I	990.0 °C Type K	990.7		Same		984.1 to 995.9 °C Type K [EMU 0.27 °C[TUR 22:1]
I	1350.0 °C Type K	1350		Same		1342.3 to 1357.7 °C Type K [EMU 0.4 °C[TUR 19:1]
Type K Probe Ch 1 Ice Point Check +/-3.4°C	0.0 °C	PASS		Same		Pass/Fail
Type K Probe Ch 2 Ice Point Check +/-3.4°C	0.0 °C	PASS		Same		Pass/Fail

Temperature: 20° C
Humidity: 52% RH
Rpt. No.: 1196675

Calibration Performed By:					Quality Reviewer:	
Panich, Eduard	331	Metrologist	847-327-5322		Ziegler, Jeff	6/7/2017
Name	ID #	Title	Phone		Name	Date

Cole-Parmer®
Delivering Solutions You Trust

Davis Instruments™

DIGI-SENSE
THE STANDARD IN PRECISION MEASUREMENT

OAKTON
INSTRUMENTS

Page 1 of 1

Appendix B   Timer documentation

Calibration complies with ISO 9001
ISO/IEC 17025 AND ANSI/NCSL Z540-1

Cert. No.: 1043-8297972

Traceable® Certificate of Calibration for 3-Button Stopwatch

Instrument Identification:

Model: 1043   S/N: 170087992   Manufacturer: Control Company

Standards/Equipment:

Description	Serial Number	Due Date	NIST Traceable Reference
Non-contact Frequency Counter	26.6 2025	3/25/17	1000389556

Certificate Information:

Technician: 150   Procedure: CAL-01   Cal Date: 2/07/17   Due Date: 2/07/19

Test Conditions: 24.6°C   59.0 %RH   1011 mBar

Calibration Data: (New Instrument)

Unit(s)	Nominal	As Found	In Tol	Nominal	As Left	In Tol	Min	Max	±U	TUR
Sec/24hr		N.A.		0.000	0.067	Y	-86.400	86.400	0.037	>4:1

This Instrument was calibrated using Instruments Traceable to National Institute of Standards and Technology.

A Test Uncertainty Ratio of at least 4:1 is maintained unless otherwise stated and is calculated using the expanded measurement uncertainty. Uncertainty evaluation includes the instrument under test and is calculated in accordance with the ISO "Guide to the Expression of Uncertainty in Measurement" (GUM). The uncertainty represents an expanded uncertainty using a coverage factor k=2 to approximate a 95% confidence level. In tolerance conditions are based on test results falling within specified limits with no reduction by the uncertainty of the measurement. The results contained herein relate only to the item calibrated. This certificate shall not be reproduced except in full, without written approval of Control Company.

Nominal=Standard's Reading;   As Left=Instrument's Reading;   In Tol=In Tolerance;   Min/Max=Acceptance Range;   ±U=Expanded Measurement Uncertainty;   TUR=Test Uncertainty Ratio;
Accuracy=±(Max-Min)/2;   Min = Nominal(Rounded) - Tolerance;   Max = Nominal(Rounded) + Tolerance;   Date=MM/DD/YY

Nicol Rodriguez
Nicol Rodriguez, Quality Manager

Aaron Judice
Aaron Judice, Technical Manager

Maintaining Accuracy:

In our opinion once calibrated your 3-Button Stopwatch should maintain its accuracy. There is no exact way to determine how long calibration will be maintained. 3-Button Stopwatchs change little, if any at all, but can be affected by aging, temperature, shock, and contamination.

Recalibration:

For factory calibration and re-certification traceable to National Institute of Standards and Technology contact Control Company.

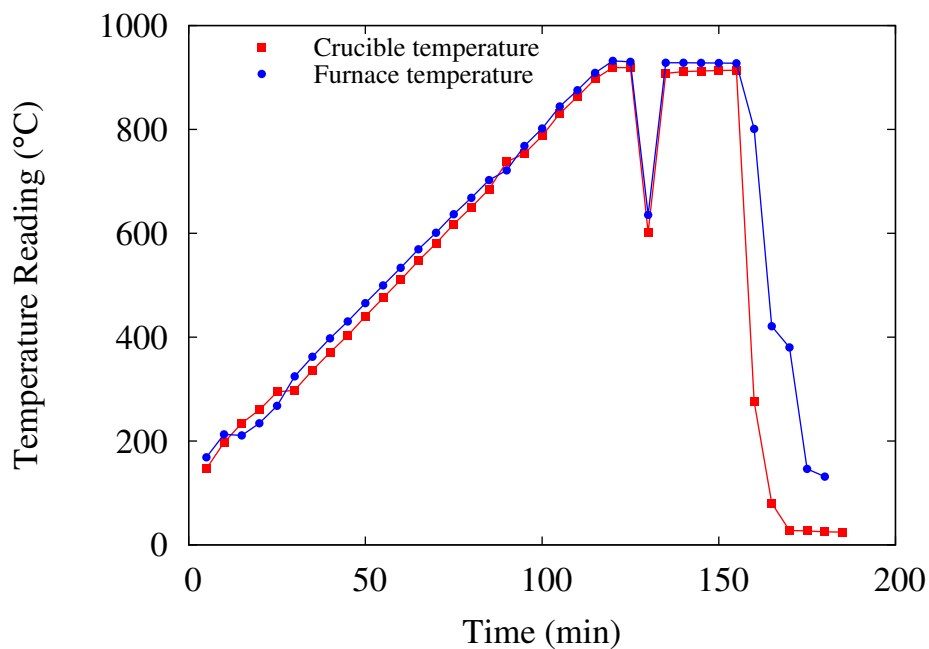# Appendix C   Furnace Baseline results

This Appendix shows the temperature profile results for the furnace baseline tests. In Figure C1, the red squares indicate the temperature from the thermocouple reader and the blue circles indicate the temperature reading from built in thermometer on the furnace. In Figures C2-C3, the red squares indicate the temperature from the thermocouple reader touching the crucible, and the blue circles indicate the temperature from the thermocouple reader that is placed in the center of the furnace cavity.
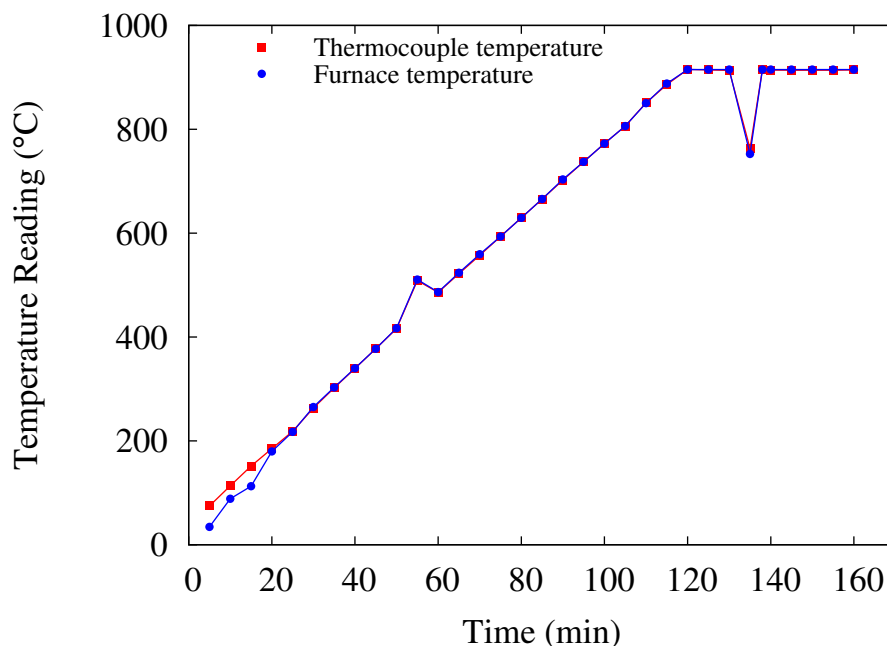
Figure C1: Furnace baseline temperature history graph, showing the thermocouple temperature of the furnace (red) and the furnace thermometer temperature (blue).
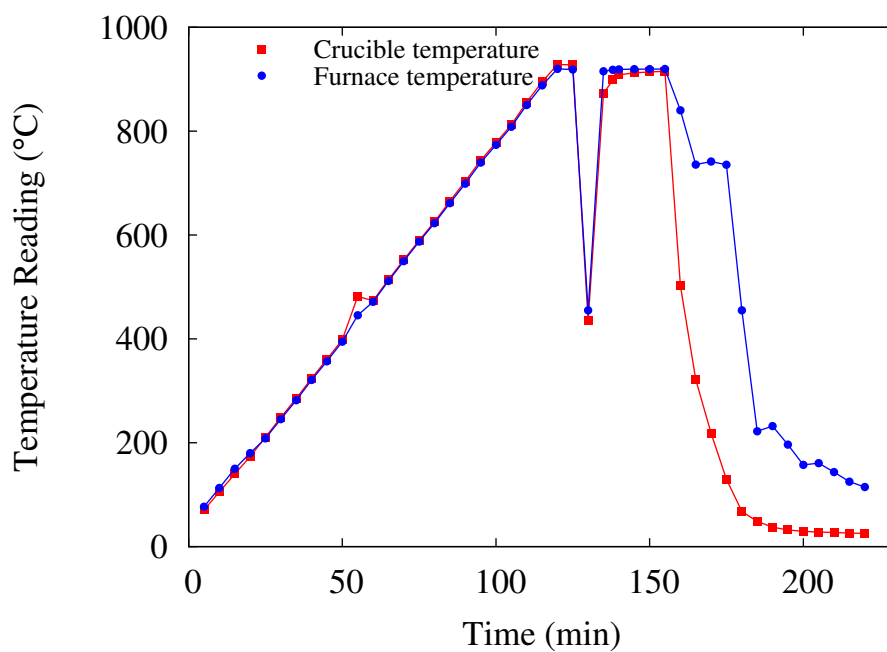
Figure C2: Alumina crucible baseline temperature history graph showing the thermocouple readings of the alumina crucible (red) and the furnace (blue).


Figure C3: Porcelain crucible baseline temperature history graph showing the thermocouple readings of the porcelain crucible (red) and the furnace (blue).

Appendix D Temperature profile results

This Appendix shows the temperature profile results for each Sample after undergoing a furnace heat treatment at its corresponding temperature. In all graphs, the furnace temperature is given in blue circles and lines, and the temperature of the crucible is given as red squares and lines.
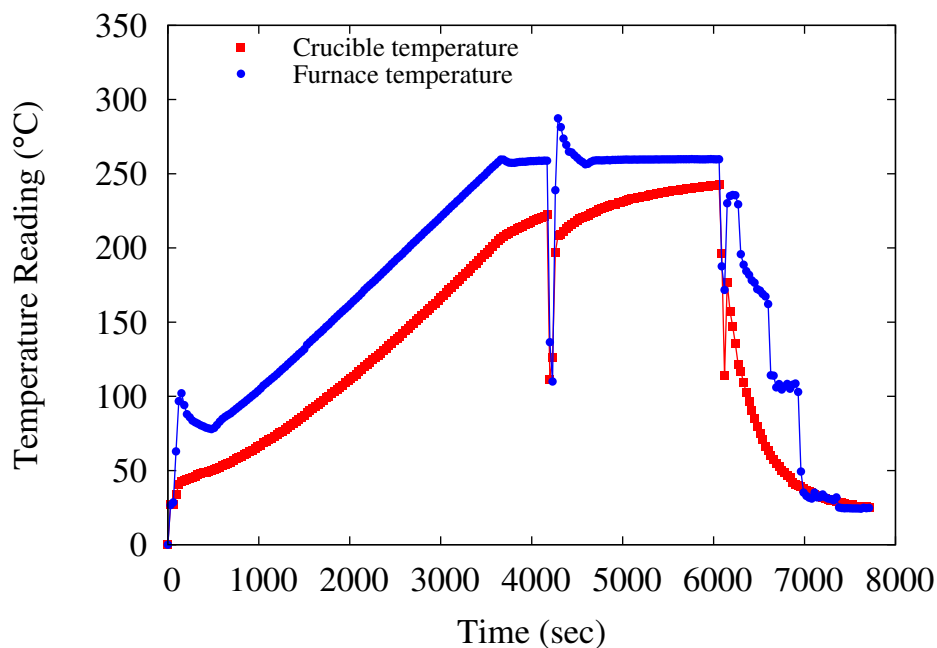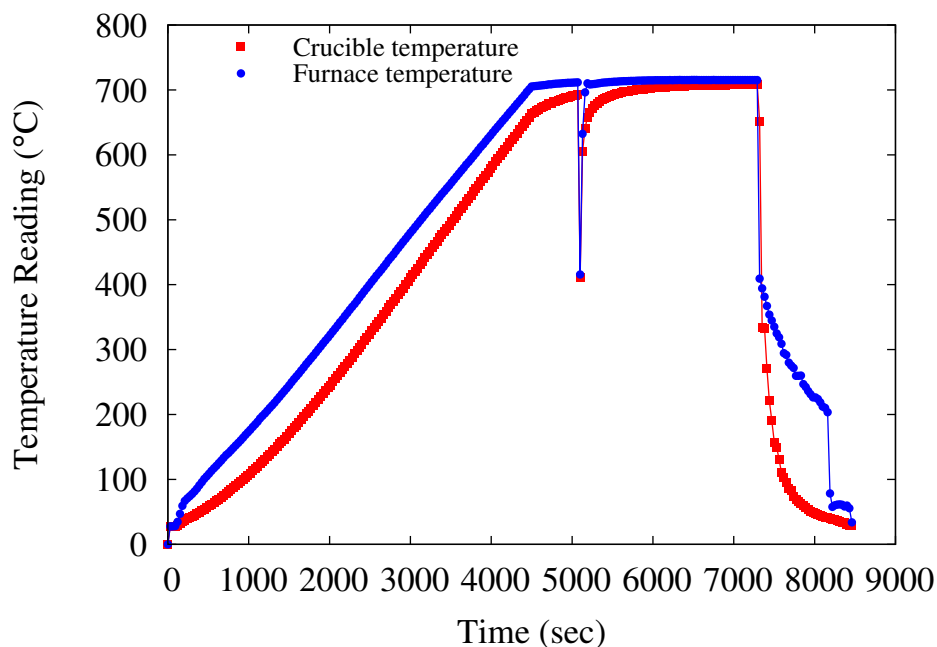

Figure D1: Temperature history profile for Sample 1A during a furnace heat treatment at 250 °C for 30 minutes, showing the furnace temperature (blue) and the temperature of the crucible containing the samples (red).
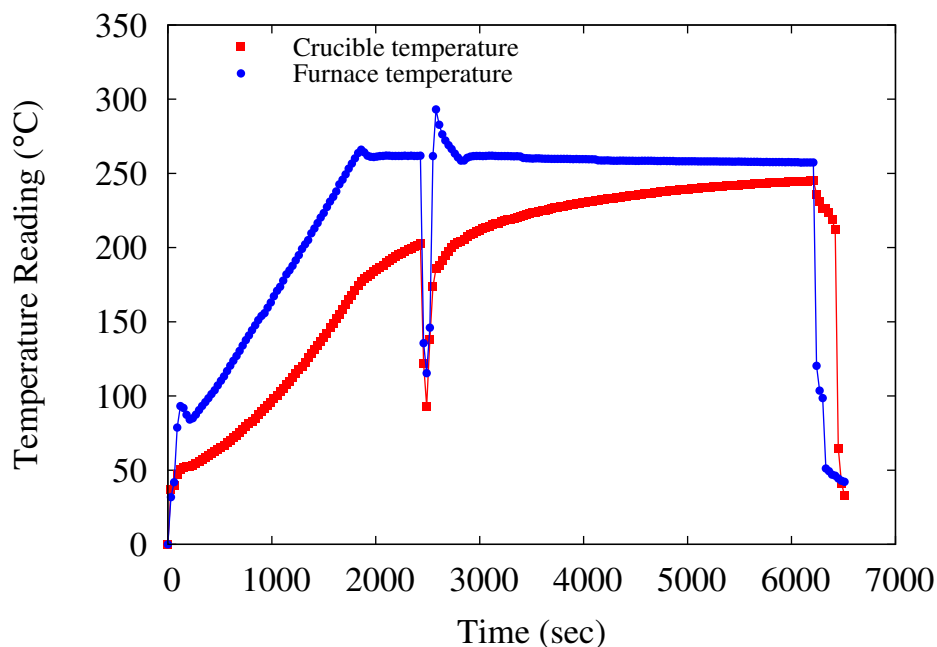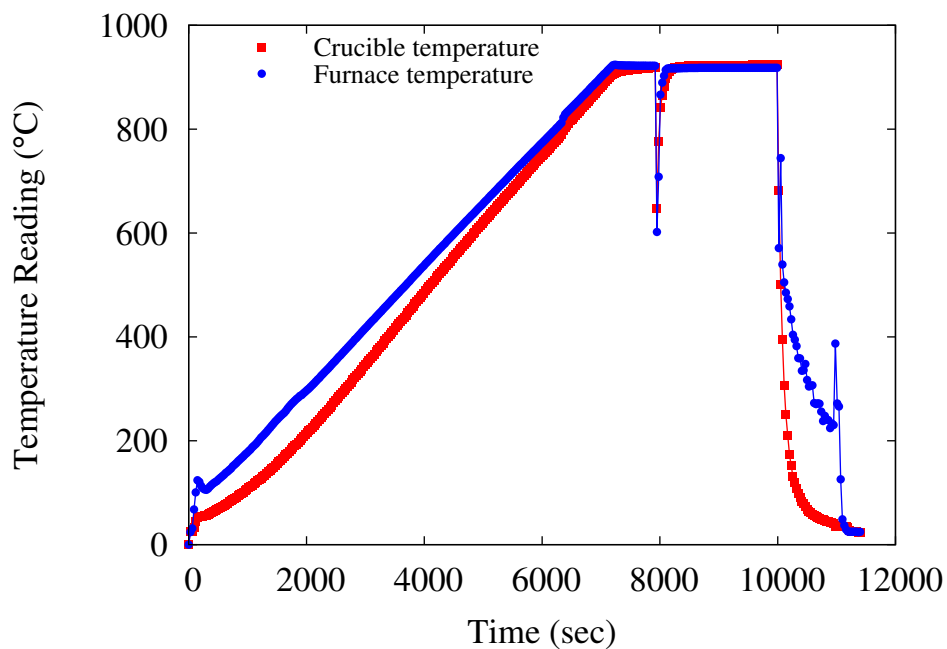
Figure D2: Temperature history profile for Sample 1B during a furnace heat treatment at 250 °C for 60 minutes, showing the furnace temperature (blue) and the temperature of the crucible containing the samples (red).
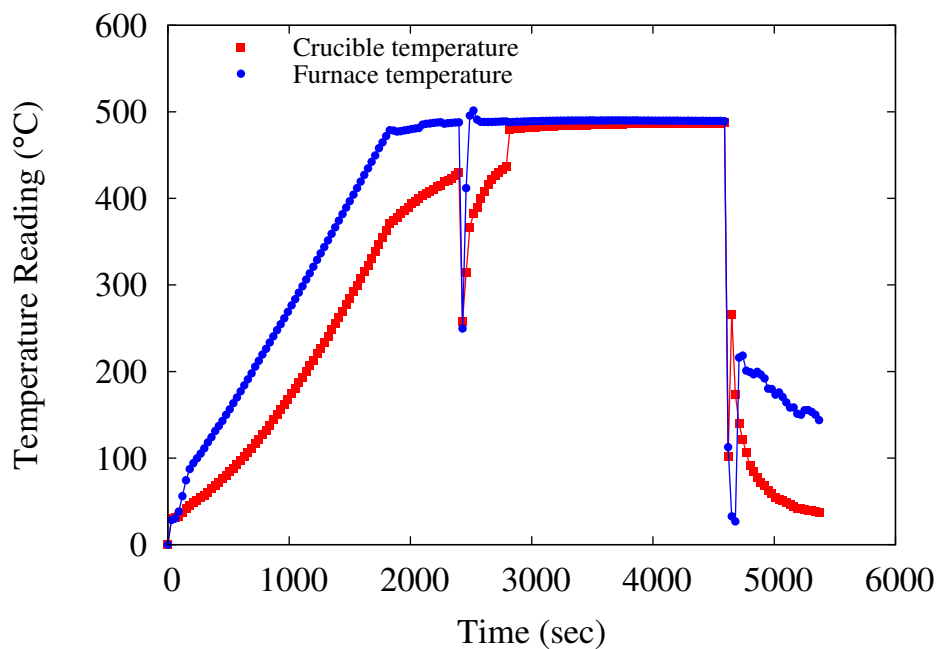
Figure D3: Temperature history profile for Sample 2 during a furnace heat treatment at 475 °C for 30 minutes, showing the furnace temperature (blue) and the temperature of the crucible containing the samples (red).

Figure D4: Temperature history profile for Sample 3 during a furnace heat treatment at 700 °C for 30 minutes, showing the furnace temperature (blue) and the temperature of the crucible containing the samples (red).

Figure D5: Temperature history profile for Sample 4 during a furnace heat treatment at 915 °C for 30 minutes, showing the furnace temperature (blue) and the temperature of the crucible containing the samples (red).

Appendix E   Additional line scans from Sample 4, heat treated at 915 °C

Figure E1 shows SEM images of Layer 1 and Layer 2 and the corresponding EDS line scans. The EDS analysis of the pewter regions shows that there is a direct correlation between tin and antimony and iron. As the counts of tin and antimony decrease, iron counts increase. Figure E1 (a) definitely shows that the dark outer region surrounding the pewter is a layer of iron. Figure E1 (b) shows that there is a region of just pewter and Figure E1 (c) shows a two-phase region.
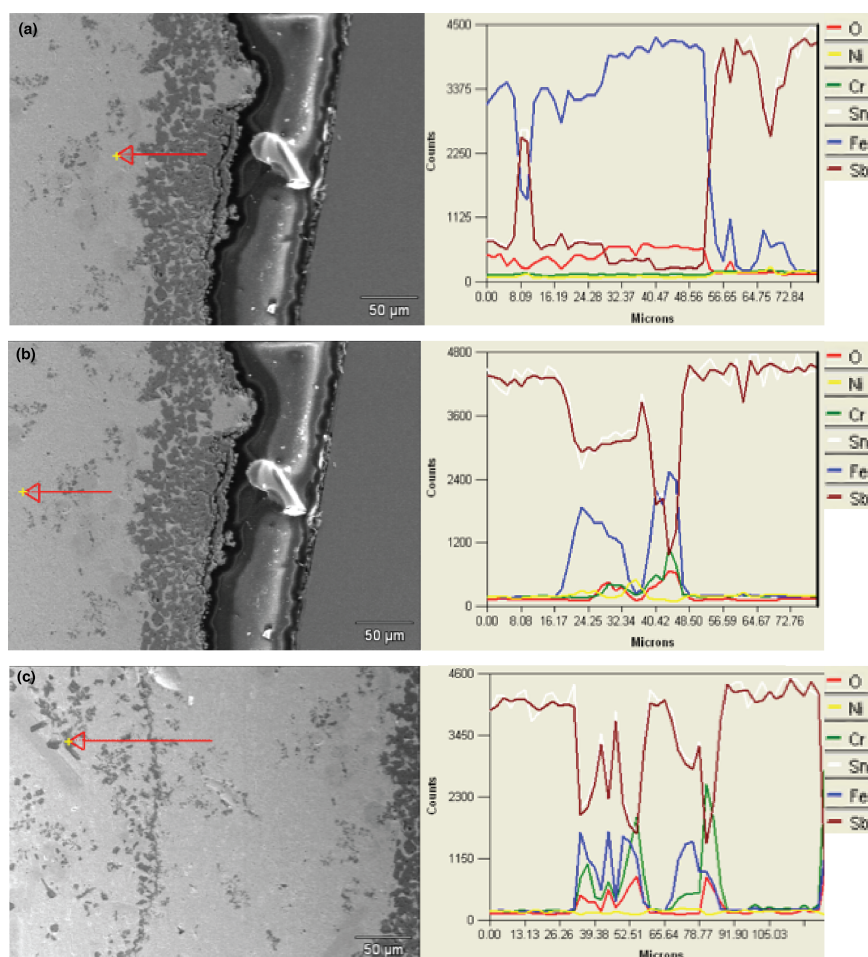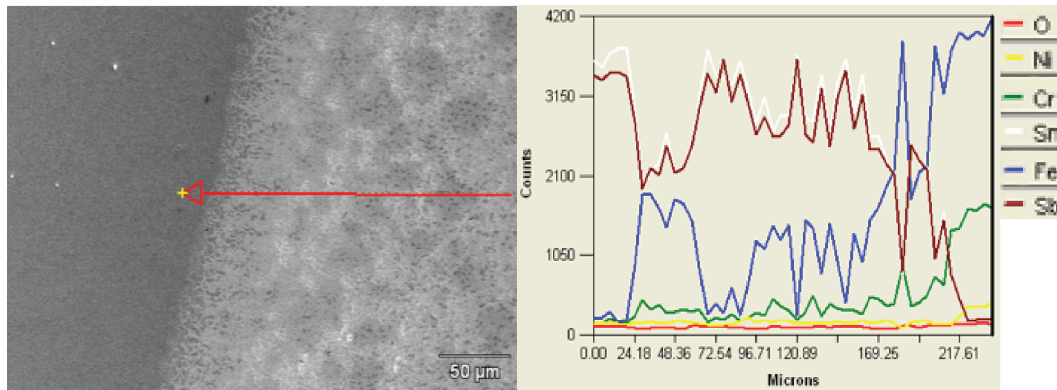

Figure E1: Higher resolution SEM image and EDS linescan of Sample 4, heat treated at 915 °C: (a) outer edge of pewter and Layer 1, (b) outer edge of pewter and Layer 1, and (c) Layer 2 and Layer 3.

The right side of the EDS line scan corresponding to Figure E2 continually shows a two-phase region. The two phase region is made up of a tin and antimony matrix with iron, chromium, and oxygen precipitates. The area of the EDS line scan between 482.95 μm to 896.88 μm is a region of just pewter and no stainless steel. Lastly, the region between the two-phase and stainless steel is the MAZ.
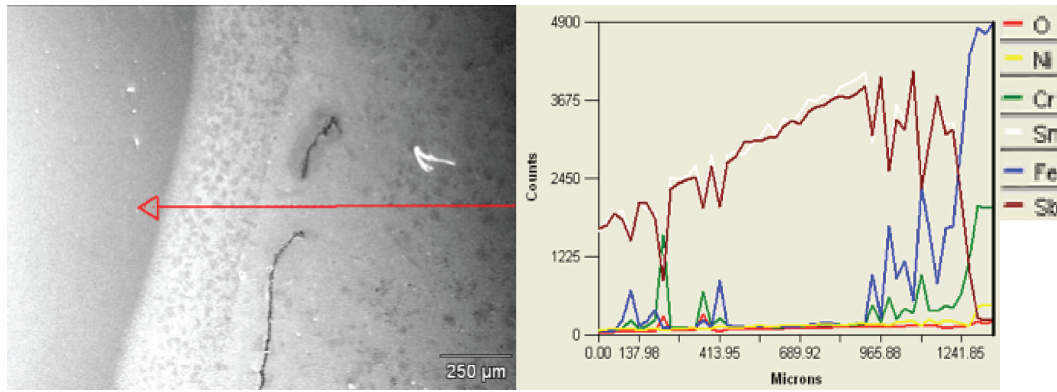
Figure E2: Higher resolution SEM image and EDS line scan of Sample 4, showing (a) the stainless steel region, Layer 5, and Layer 4.

A closer look at Layer 5, the MAZ can be seen in Figure E3 along with its corresponding EDS line scan. According to the EDS line scan, the MAZ is comprised of tin and antimony and a larger count of iron and chromium than that in the diluted region from Figure E2. This suggests that pewter is penetrating into the stainless steel.

Figure E3: Higher resolution SEM image and EDS line scan of Sample 4, showing Layer 5, the MAZ.